Folded Reflectarrays with Shaped Beam Pattern for Foreign Object Debris Detection on Runways

Armin Zeitler, Jérôme Lanteri, Christian Pichot, Claire Migliaccio, Peter Feil, and Wolfgang Menzel, *Fellow, IEEE*

***Abstract*—This paper describes the design of a folded reflectarray antenna (FRA) by phase only control to provide a cosecan squared beam pattern in elevation and a pencil-beam pattern in azimuth to detect objects on the ground, e. g. on runways. A very compact folded reflectarray antenna was fabricated and its radiation pattern over frequency was simulated. During the design process a conical horn was developed, which illuminates the array, with symmetrical radiation pattern for all planes and for a frequency range of 76 to 81 GHz. As the FRA consists of a single layer substrate this kind of antenna could be a candidate for low-cost production in FOD detection on airports in the future.**

I. Introduction

THE detection of **F**oreign **O**bject **D**ebris (FOD) on airports becomes more and more important. A basic motivation is the fatal accident with a Concorde aircraft a few years ago due to a metal part lost by an aircraft on the runway some time before. Up to now only two systems are successful in field worldwide [1], [2].

A previous study conducted on FOD detection on runways [3] has shown that very small objects could be detected with an already existing compact mm-wave front-end in combination with a narrow beam antenna. Now further considerations should be done in order to increase the sensitivity for detection. For this reason and to maintain a compact system a folded reflectarray was chosen, which provides a cosecan squared pattern in elevation and a pencil-beam radiation pattern in azimuth. In the past beamforming was done between 24.5 and 26.5 GHz with a multilayer structure [4] and by phase and amplitude distribution in the 60 GHz band [5] with one layer. In the following case, the design is pushed to mm-wave frequency of 78 GHz with a 5 GHz bandwidth and is done by phase only control. An optimisation routine is used based on the method described in [5], but simplified to one dimension, which means that the design and optimisation can be achieved very fast even for large reflectarrays. The resulting far field was simulated based on a two dimensional Fourier transformation over a frequency range of 5 GHz. The single layer structure is easy to fabricate for low-cost and mass-production compared to multilayer proposals [4], [6]. As a very compact FRA is used, we have to pay particular attention to the radiation pattern of the primary feed that has to be constant over frequency and symmetrical for all planes.

In section II the system requirements are introduced, and based on them the one dimensional design process, the expansion to the second dimension as well as the design of the primary feed are derived. Then the used optimisation routine is explained in section III. The results of the simulations and of the measurements over the whole frequency band of interest are presented in section IV. Finally the conclusions will be addressed in section V.

A. Zeitler, J. Lanteri, C. Pichot and Claire Migliacccio are with the Department of Laboratoire d'Electronique Antennes et Télécommunications, 250 Rue Albert Einstein, 06560 Valbonne, France, e-mail: armin.zeitler@unice.fr.

P. Feil and W. Menzel are with the Institute of Microwave Techniques, University of Ulm, Albert-Einstein-Allee 41, 89081 Ulm, Germany, e-mail: peter.feil@uni-ulm.de.

II. System Requirements and Design Approach

A. System Requirements

The application of interest is shown in Fig. 1 with its requirements in TABLE I. In any monostatic radar system

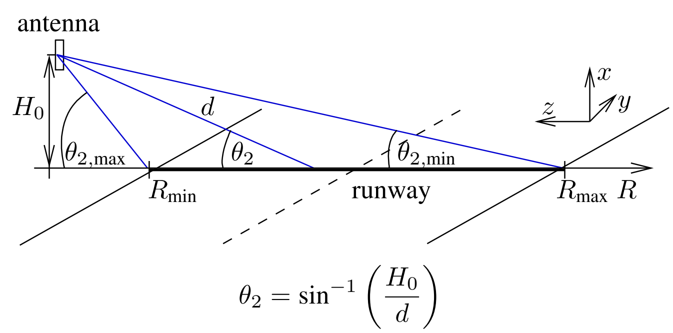

Fig. 1. Scenario for detecting objects on the runway.

TABLE I
System requirements for the antenna design.

Name	Value	Description
H_0	0.5 m	Height sensor over runway
$R_{\min}$	0.8 m	Minimal distance between sensor and runway
$R_{\max}$	100.0 m	Maximum distance between sensor and runway
$\theta_{2,\min}$	0.3°	Minimum angle in elevation
$\theta_{2,\max}$	32.0°	Maximum angle in elevation

the received power is $P_{\mathrm{RX}} \sim {}^{G(\theta_2)^2}/_{d^4}$. Antennas with a cosecan squared pattern are a solution to achieve a constant received power within a distance range $[R_{\min}, R_{\max}]$. In the azimuth a pencil-beam pattern is used because the antenna will be scanned mechanically.

B. One Dimensional Design Approach

The reflective array as in Fig. 2 is designed to provide a cosecan squared pattern $G_2(\theta_2)$ in the x-z-plane and a

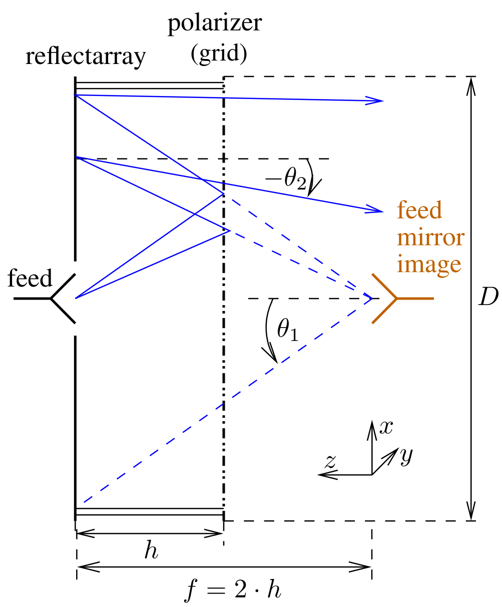

Fig. 2. Folded antenna setup and definition of focal length f.

pencil-beam pattern in the y-z-plane. The primary source radiates with a given antenna pattern $G_1(\theta_1)$. The radiation of the primary source in elevation is described by $\theta_{1,x}$ and in azimuth by $\theta_{1,y}$. As a symmetrical radiation pattern of the primary source is assumed, $\theta_{1,x} = \theta_{1,y} = \theta_1$ can be defined. The radiated power density in the respective far field is $U_1(\theta_1) \sim G_1(\theta_1)$ and $U_2(\theta_2) \sim G_2(\theta_2)$. Assuming a line source towards y as primary source the following equation has to be valid due to energy conservation:

$$\int_{\theta_{1,\text{min}}}^{\theta_1} U_1(\theta_1) d\theta_1 = C \cdot \int_{\theta_2}^{\theta_{2,\text{max}}} U_2(\theta_2) d\theta_2 \qquad (1)$$

The constant C ensures that the radiated power of the feed and that of the desired radiation pattern are equal in the angular range of interest. The numerical solution of (1) leads to $\theta_2 = f(\theta_1)$.
In x direction i gives the discrete position of each cell ($i \in [1..M]$), the same is done in y direction by j ($j \in [1..N]$). With the orientation of the angles θ_1 and θ_2 on the reflector surface as in Fig. 2, the derivation of the phase shift ϕ in one dimension is calculated according to [7], where k is the wave number ${}^{2\pi}/_{\lambda}$:

$$\frac{\partial \phi}{\partial x} = -\, k \cdot [\sin(\theta_1) + \sin(\theta_2)] \qquad (2)$$

$$\Rightarrow \phi_{\text{cosecans}}(i) = \left[\phi_{\text{cosecans}}(1), \cdots, \phi_{\text{cosecans}}(M)\right] \qquad (3)$$

To provide a pencil-beam pattern, the required phase shift in the azimuth is done by compensation of the phase delay $\phi_{\text{delay}}(y)$, (5), which is introduced by free space propagation.

$$\phi_{\text{delay}}(y) = -\, k \cdot \frac{f}{\cos(\theta_1)} \qquad (4)$$

$$\phi_{\text{pencil}}(y) + \phi_{\text{delay}}(y) = 0 \qquad (5)$$

$$\Rightarrow \phi_{\text{pencil}}(j) = \begin{bmatrix} \phi_{\text{pencil}}(1) \\ \vdots \\ \phi_{\text{pencil}}(N) \end{bmatrix} \qquad (6)$$

Knowing the reflection phase on the reflector surface ($\phi_{\text{cosecans}}(i)$ and $\phi_{\text{pencil}}(j)$) the overall phase of the electrical field can be calculated by adding $\phi_{\text{delay}}(i)$ or $\phi_{\text{delay}}(j)$ respectively for each dimension separately, where $\phi_{\text{delay}}(x) = \phi_{\text{delay}}(y)$ due to the symmetry of the antenna.

$$\Phi_{\text{cosecans}}(i) = \phi_{\text{cosecans}}(i) + \phi_{\text{delay}}(i) \qquad (7)$$

$$\Phi_{\text{pencil}}(j) = \phi_{\text{pencil}}(j) + \phi_{\text{delay}}(j) \qquad (8)$$

In this special case of a pencil-beam pattern in the azimuth, Φ_{pencil} includes zero or a constant value for all entries of the vector as $\phi_{\text{pencil}}(y) = -\phi_{\text{delay}}(y)$.

C. Two Dimensional Expansion

To get the phase distribution $\Phi_{\text{tot}}(i,j)$ of the electrical field in two dimensions, $\Phi_{\text{cosecans}}(i)$ must be replicated N-times for each row and $\Phi_{\text{pencil}}(j)$ M-times for each column. Following this, the two resultant matrices have to be added. Finally one gets the reflection phase $\phi_{\text{reflector}}(i,j)$ of the reflector by subtracting the free space delay $\phi_{\text{delay}}(i,j)$ from the desired phase $\Phi_{\text{tot}}(i,j)$ (10).

$$\phi_{\text{delay,real}}(x,y) = -k \cdot \sqrt{x^2 + y^2 + f^2} \qquad (9)$$

$$\begin{matrix}\phi_{\text{reflector}} \\ (i,j)\end{matrix} = \begin{bmatrix} \ddots & & \iddots \\ & \begin{matrix}\Phi_{\text{tot}} \\ (i,j)\end{matrix} & \\ \iddots & & \ddots \end{bmatrix} - \begin{bmatrix} \ddots & & \iddots \\ & \begin{matrix}\phi_{\text{delay,real}} \\ (i,j)\end{matrix} & \\ \iddots & & \ddots \end{bmatrix} \qquad (10)$$

With the two dimensional phase distribution on the reflector one can simulate the radiation pattern with an equivalent aperture method [8].

D. Primary Feed Design

As the expansion to the second dimension is done implicitly considering an axially symmetric primary feed, the resulting radiation pattern has to be symmetrical for all planes. Additionally the design process of the antenna aimed at achieving an aperture efficiency ϵ_{ap} according to [9] and [10] $\epsilon_{\text{ap}} \sim \epsilon_{\text{t}} \cdot \epsilon_{\text{s}}$, with the taper efficiency ϵ_{t} and spillover efficiency ϵ_{s}, as high as possible. A small circular horn is a good candidate which fulfils the conditions mentioned above provided that some steps [11] were added. The horn was designed with SRSRD [12] which is an in-house software, developed by France Telecom, Orange Labs in La Turbie, France. The simulation results of the radiation pattern for 78 GHz in the 45°-plane were finally used for the design and optimisation process of the reflectarray and replaced the mathematical model of the primary source $G(\theta_1) = \cos^{10}(\theta_1)$. The exponent $n = 10$ of the cosine is a trade-off in having a small diameter and a directive radiation pattern of the horn. It was fabricated and measured (Fig. 3). The gain of the conical horn is 13.6 dB at 78 GHz which is close to the simulated one of 13.3 dB. In order to improve the radiation pattern measurements and to suppress ripples due to the anechoic chamber at mm-waves, a classical digital filtering was employed. The measured radiation pattern is almost constant over frequency, which was one of the design goals.

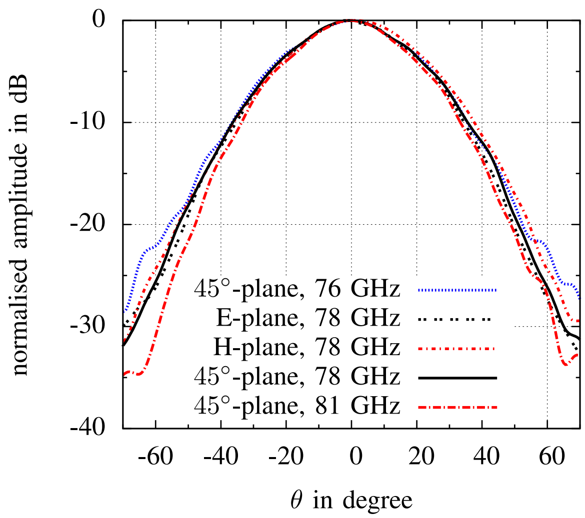

Fig. 3. Measured and filtered radiation pattern of the primary feed in the E-, H- and 45°-plane for 78 GHz and in the 45°-plane for 76 and 81 GHz.

III. Optimisation

The design procedure and the far field simulation for one dimension were implemented using Scilab [13]. The primary source pattern was modelled as $G(\theta_1) = \cos^n(\theta_1)$. The design frequency was 78 GHz. The design comes with three degrees of freedom: diameter D, height of the antenna h and the integer n. A reduction of D and n led to a degradation of the resulting radiation pattern as shown in Fig. 4. To avoid this, a non-linear optimisation routine was used, as the target function is non-linear. As algorithm the Newton's method was chosen. Therefore the mean absolute error between the resulting and desired radiation patterns was calculated as the error function to be minimised with the build-in function *optim* of Scilab. The optimisation includes the following steps:

- Calculation of the resulting radiation pattern in the cosecan squared plane with the calculated phase- and amplitude distributions on the reflector surface for one dimension based on the array factor.
- Calculation of the gain $G(\theta_2)$ and normalisation with respect to the overall radiated power.
- Mean absolute error between the desired and the resulting directivity represents the cost function, which is used as input for the *optim* function of Scilab.

With the optimisation it is possible to design an antenna with smaller diameter D in combination with a less directive primary source.

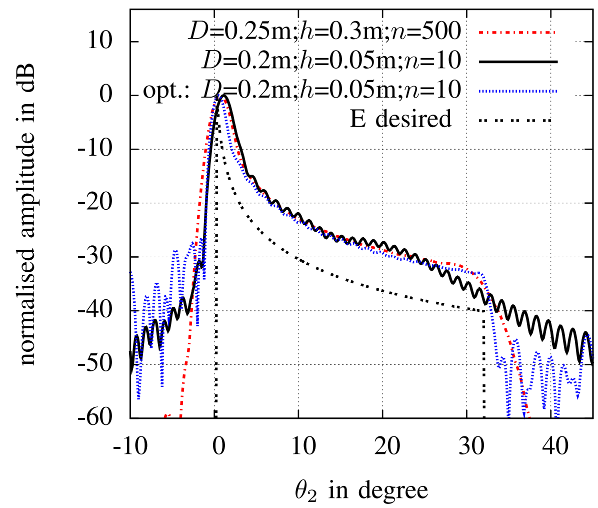

Fig. 4. Simulation results: cosecan squared pattern in elevation.

IV. Simulation of the Radiation Pattern over Frequency and Comparison with Measurements

The dimensions of the fabricated folded reflectarray antenna are listed in Tab. II. The values of ϵ_{s}, ϵ_{t} and ϵ_{ap} were calculated excluding the grid influence (see Fig. 2). The dimensions of the used patches were calculated according to [5] and were given for 78 GHz. In order to simulate qualitatively the radiation pattern of the antennas for a frequency range from 76 to 81 GHz, the behaviour over frequency of the patches has to be known. Therefore a Unit Cell **W**ave**G**uide**A**pproach (WGA) [14] was done, and every isolated patch was simulated with Ansoft HFSS [15]. These results were used as input for the simulation of the radiation pattern with Scilab. In addition the variation of the radiation pattern and the variation of phase with respect to the point assumed as phase centre of the primary source (simulated with SRSRD) were taken into account. The FRA has been assembled and the gain measured. Results are shown in Fig. 5. The aperture efficiency is classically defined as:

TABLE II
Dates of fabricated reflector.

Diameter D	Height h	ϵ_{s}	ϵ_{t}	ϵ_{ap}
0.12 m	0.0325 m	96.63 %	77.18 %	74.57 %

$$\epsilon_{\mathrm{ap}} = \frac{G_{\mathrm{measured}}}{\left(\frac{\pi \cdot D}{\lambda}\right)^2} \tag{11}$$

$\left({}^{\pi D}/_{\lambda}\right)^2$ in (11) represents the maximum gain of a planar aperture under constant illumination. The maximum gain is 36.0 dB for 77.3 GHz. This results in a maximum efficiency of 42 %, which still remains a state-of-the-art value at this frequency. Measurements of the radiation pattern of the antenna were conducted between 76 and 81 GHz. The definition of the planes is shown in Fig. 6. The first side lobe level in the pencil-beam plane is below -15 dB for the frequency

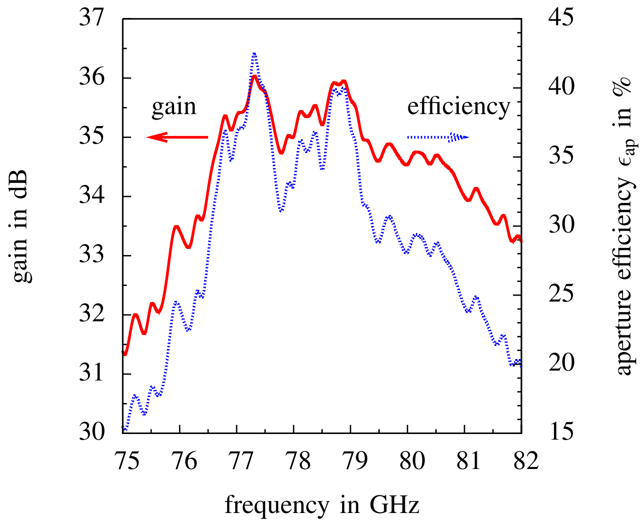

Fig. 5. Measured gain and resulted aperture efficiency.

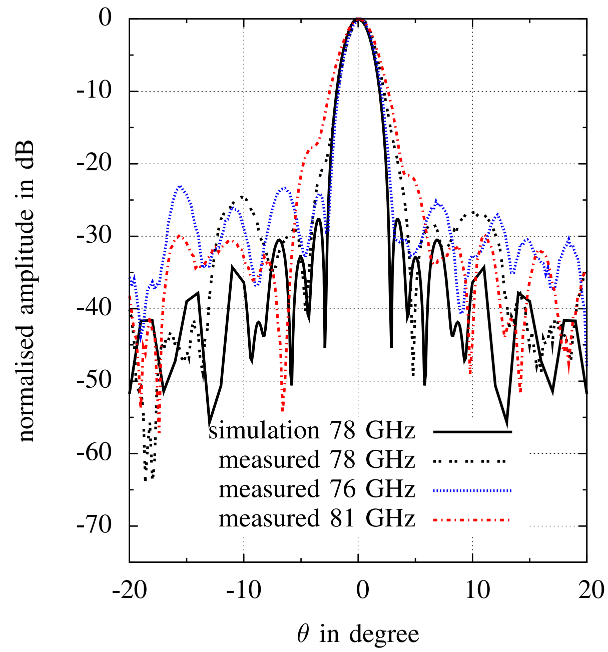

Fig. 7. Comparison of the measured (76, 78, 81 GHz) and simulated (78 GHz) radiation pattern in the pencil-beam plane.

range of interest. Beam width is less than 2.8° as shown in Fig. 7. In the cosecans plane, very good agreement is obtained between the simulation results and the measured ones for the design frequency of 78 GHz (Fig. 8) as well as for 76 GHz and 81 GHz respectively. The received power P_{RX}

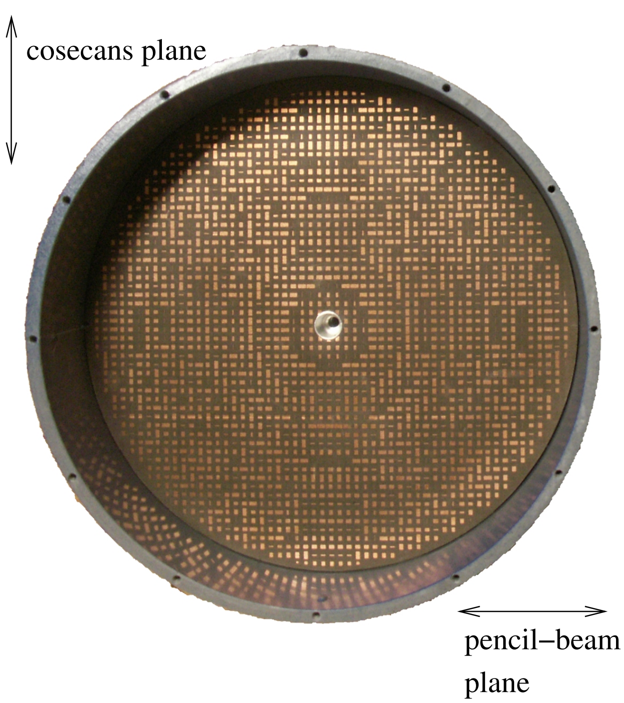

Fig. 6. Inlay of the antenna with the primary feed and definition of the planes.

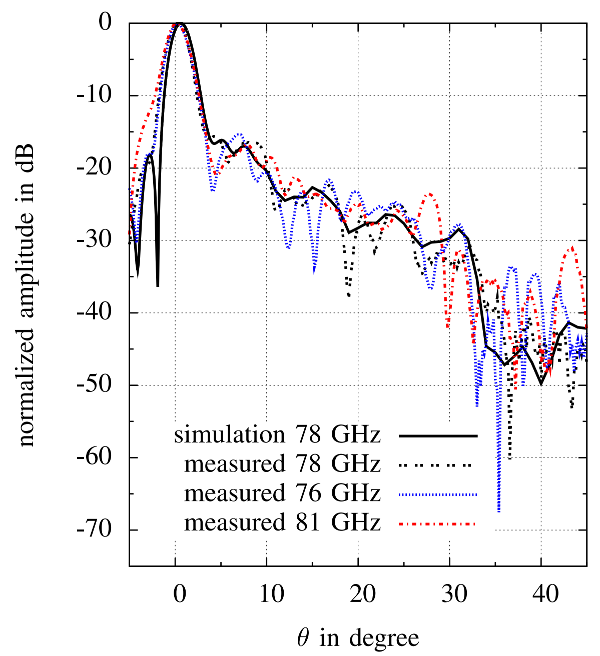

Fig. 8. Comparison of the measured (76, 78, 81 GHz) and simulated (78 GHz) radiation pattern in the cosecan^2 plane.

calculated out of the radiation pattern measured in the cosecans plane as function of the distance R varies about 37 dB over the considered frequency range. Assuming an antenna with a constant gain for all θ_2, the variation in power would be more than 80 dB.

V. Conclusion

The design described above is done one dimensional and in elevation and azimuth separately, therefore, it can be conducted very fast compared to full wave simulation programmes. This is true also for the involved optimisation process. A conical horn including three steps provides an almost symmetrical radiation pattern, which is also nearly constant over a bandwidth of 5 GHz. This enables the realisation of a folded reflectarray antenna for the frequency range of 76 to 81 GHz. Simulations of the frequency behaviour of the reflected phase of each isolated patch were done to predict the radiation pattern of the array antenna. Measurements verify the capability of this approach. The antenna consists of a single layer structure and was fabricated with classical printed circuit board techniques. This allows an easy production, which is an important advantage regarding low-cost and large-scale production.

REFERENCES

[1] QinetiQ. (2009) Tarsier - QinetiQ automatic runway debris detection. [Online]. Available: http://www.qinetiq.com/home/products/tarsier.html

[2] Xsight. (2009) Xsight - Advanced radar and optic sensors for FOD detection and homeland security. [Online]. Available: http://www.xsightsys.com/

[3] P. Feil, W. Menzel, T. Nguyen, C. Pichot, and C. Migliaccio, "Foreign objects debris detection (fod) on airport runways using a broadband 78 ghz sensor," in *Proc. EURAD 2008*, Amsterdam, Netherlands, Oct. 2008.

[4] J. A. Zornoza, R. Leberer, J. A. Encinar, and W. Menzel, "Folded multilayer microstrip reflectarray with shaped pattern," *IEEE Trans. Antennas Propag.*, vol. 54, pp. 510–518, 1363, Feb. 2006.

[5] R. Leberer and W. Menzel, "A dual planar reflectarray with synthesized phase and amplitude distribution," *IEEE Trans. Antennas Propag.*, vol. 53, pp. 3534–3539, Nov. 2005.

[6] A. Vallecchi and G. B. Gentili, "A low-cost shaped-beam hybrid-feed microstrip planar array antenna for x-band polarimetric radar systems," *Radar Conference, 2006, EuRAD 2006, 3rd European*, pp. 124–127, Sep. 2006.

[7] W. Menzel, D. Pilz, and M. Al-Tikriti, "Millimeter-wave folded reflector antennas with high gain, low loss, and low profile," *IEEE Trans. Antennas Propag.*, vol. 44, pp. 24–29, Jun. 2002.

[8] J. Lanteri, C. Migliaccio, J.-Y. Dauvignac, and C. Pichot, "Reflectarray using an offset prolate feed at 94 ghz," *Antennas and Propagation Society International Symposium*, pp. 1–4, Jul. 2008.

[9] D. M. Pozar, S. D. Targonski, and H. D. Syrigos, "Design of millimeter wave microstrip reflectarrays," *IEEE Trans. Antennas Propag.*, vol. 45, pp. 287–296, Feb. 1997.

[10] C. A. Balanis, *Antenna Theory, Second Edition, Analysis and Design*. John Wiley & Sons, Inc., 1997.

[11] S. Drabowitch, A. Papiernik, H. D. Griffiths, J. Encinas, and B. L. Smith, *Modern Antennas, Second Edition*. Springer, 2005.

[12] A. Berthon and R. P. Bills, "Integral equation analysis of radiating structures of revolution," *IEEE Trans. Antennas Propag.*, vol. 37, pp. 159–170, Feb. 1989.

[13] Scilab. (2008) The scilab website. [Online]. Available: http://www.scilab.org/

[14] F. E. Tsai and M. E. Bialkowski, "An equivalent waveguide approach to designing of reflect arrays with the use of variable-size microstrip patches," *Microwave and Optical Technology Letters*, vol. 34, pp. 172–175, Jun. 2002.

[15] Ansoft. (2008) HFSS 3D EM Simulation Software for RF, Wireless, Packaging and Optoelectronic Design. [Online]. Available: http://www.ansoft.com/products/hf/hfss/